World Journal of Diabetes

Submit a Manuscript: https://www.f6publishing.com

*World J Diabetes* 2022 August 15; 13(8): 622-642

DOI: 10.4239/wjd.v13.i8.622

ISSN 1948-9358 (online)

ORIGINAL ARTICLE

Basic Study

# *In vivo* evaluation and mechanism prediction of anti-diabetic foot ulcer based on component analysis of Ruyi Jinhuang powder

Xiu-Yan Li, Xiao-Tong Zhang, Yi-Cheng Jiao, Hang Chi, Ting-Ting Xiong, Wen-Jing Zhang, Mi-Nan Li, Yan-Hong Wang

**Specialty type:** Endocrinology and metabolism

**Provenance and peer review:** Unsolicited article; Externally peer reviewed.

**Peer-review model:** Single blind

**Peer-review report's scientific quality classification**

Grade A (Excellent): A
Grade B (Very good): B, B
Grade C (Good): 0
Grade D (Fair): 0
Grade E (Poor): 0

**P-Reviewer:** Bahrmann A, Germany; Elnakib AA, Egypt; Lee AS, Australia

**Received:** May 6, 2022
**Peer-review started:** May 6, 2022
**First decision:** May 30, 2022
**Revised:** June 10, 2022
**Accepted:** July 6, 2022
**Article in press:** July 6, 2022
**Published online:** August 15, 2022

**Xiu-Yan Li, Yi-Cheng Jiao, Hang Chi, Ting-Ting Xiong, Wen-Jing Zhang, Mi-Nan Li, Yan-Hong Wang,** Key Laboratory of Basic and Application Research of Beiyao, Heilongjiang University of Chinese Medicine, Harbin 150040, Heilongjiang Province, China

**Xiu-Yan Li,** College of Pharmacy, Harbin Medical University, Harbin 150040, Heilongjiang Province, China

**Xiao-Tong Zhang,** Key Laboratory of Basic and Application Research of Beiyao, Heilongjiang University of Chinese Medicine, Ministry of Education, College of Pharmacy, Harbin 150040, Heilongjiang Province, China

**Corresponding author:** Yan-Hong Wang, MD, Teacher, Key Laboratory of Basic and Application Research of Beiyao, Heilongjiang University of Chinese Medicine, No. 24 Heping Road, Xiangfang District, Harbin 150040, Heilongjiang Province, China. 799378826@qq.com

## Abstract

### *BACKGROUND*

Diabetes is a metabolic disease with a high complication rate. Diabetic foot ulcers (DFUs) seriously affect the quality of life of patients. A total of 15%-20% of diabetic patients develop DFUs, which heal with difficulty over a long time and can result in amputation and disability. Traditional Chinese medicine has a unique effect in the treatment of skin ulcerative diseases. Ruyi Jinhuang powder (RHP) is one of the classic prescriptions in traditional Chinese medicine and is widely used in clinical practice.

### *AIM*

To verify the ability of RHP to promote wound healing by electron microscopy analysis in animal models and hematoxylin-eosin (HE) staining. The effective components of RHP were extracted and identified by gas chromatography-mass spectrometry (GC-MS), and the obtained chemical components were analyzed by network pharmacology methods to predict its therapeutic mechanism.

### *METHODS*

Sprague Dawley rats were injected with streptozotocin to establish the DFU model. HE staining was used to observe the wound tissue under an electron microscope. The chemical constituents of RHP were extracted first by supercritical fluid extraction and alcohol extraction, and then, GC-MS and ultra-performance

liquid chromatography–MS were used to separately identify the chemical constituents. In addition, the "herb-component-target" link was established through the Traditional Chinese Medicine Systems Pharmacology database to obtain the target information, and the molecular docking of important components and key targets was performed in Discovery Studio software. Cytoscape software was used to visualize and analyze the relationship between the chemical composition, targets and Traditional Chinese Medicine network.

***RESULTS***

RHP promoted DFU healing in rats by affecting fibroblasts and nerve cells. A total of 89 chemical components were obtained by GC-MS. Network pharmacological analysis revealed that RHP was associated with 36 targets and 27 pathways in the treatment of DFU, of which the important components were luteolin, trans caryophyllene, ar-turmerone, palmitic acid, methyl palmitate, gallic acid, demethoxycurcumin, berberine, and rheic acid. The key targets were posttranscriptional silencing, topoisomerase II alpha, muscarinic acetylcholine receptor M2, interleukin 6, tumor necrosis factor and retinoic X receptor alpha, and the key pathways were the phosphoinositide 3-kinase-protein kinase B signaling pathway, neuroactive ligand–receptor interactions, and the forkhead box O signaling pathway.

***CONCLUSION***

Our results indicated that RHP may play a role in the treatment of DFU through these target pathways by affecting insulin resistance, altering the nervous system and immune system, participating in inflammatory responses and regulating cell proliferation, differentiation and apoptosis through other specific mechanisms.

**Key Words:** Ruyi Jinhuang powder; Diabetic foot ulcer; Mass spectrometry-chromatography; Network pharmacology; Hematoxylin-eosin staining; Components analysis



**Core Tip:** Although some studies have suggested that Ruyi Jinhuang powder (RHP) has a therapeutic effect on diabetic foot ulcers (DFUs), few have used component analysis, investigated the mechanism of action, and utilized wound-healing experiments. The components of RHP were used to predict the mechanism of action, and wound healing was observed by establishing a DFU rat model to further prove the therapeutic effect of RHP on DFU to finally determine a possible mechanism of action.

**Citation:** Li XY, Zhang XT, Jiao YC, Chi H, Xiong TT, Zhang WJ, Li MN, Wang YH. *In vivo* evaluation and mechanism prediction of anti-diabetic foot ulcer based on component analysis of Ruyi Jinhuang powder. *World J Diabetes* 2022; 13(8): 622-642

**URL:** https://www.wjgnet.com/1948-9358/full/v13/i8/622.htm

**DOI:** https://dx.doi.org/10.4239/wjd.v13.i8.622

## INTRODUCTION

Ruyi Jinhuang powder (RHP) is included in "Authenticity of Surgery" written by Chen Shigong in the Ming Dynasty, which includes "*THF* [*Trichosanthin* (*Tian Hua Fen*)], *DH* [*Rhubarb* (*Da Huang*)], *HB* [*Phellodendron* (*Huang Bai*)], *JH* [*Turmeric* (*Jiang Huang*)], *BZ* [*Angelica dahurica* (*Bai Zhi*)], *TNX* [*Arisaema* (*Tian Nan Xing*)], *CZ* [*Atractylodes lancea* (*Cang Zhu*)], *HP* [*Magnolia officinalis* (*Hou Po*)], *CP* [*Pericarpium Citri Reticulatae* (*Chen Pi*)] and *GC* [*Glycyrrhiza uralensis* (*Gan Cao*)]"[1] and is now included in the Chinese Pharmacopoeia. This prescription is used for swelling relief and pain relief. In this prescription, *Trichosanthes* is the monarch medicine, and the minister medicine *rhubarb* with the same cold and bitter taste is used to purge fire detumescence; *angelica dahurica* and *turmeric* are the minister pungent medicines with compatibility to discharge pus pain; *pericarpium citri reticulatae*, *Magnolia officinalis*, *atractylodes lancea and glycyrrhiza uralensis* are combined to remove dampness and regulate Qi; and *arisaema* alleviates swelling pain. The above five medicines act together as adjuvants with *glycyrrhiza uralensis* to reconcile and detoxify the medicine. Modern clinical applications mainly include cutaneous vasculitis, gouty arthritis, herpes zoster and diabetic foot ulcer (DFU). After many studies on its pharmacological effects, it was found that RHP can inhibit bacterial infection, increase lysosomal content, enhance immune defenses and inhibit inflammation. The traditional preparation is through the addition of honey to the powder, which is then directly applied to the affected area to treat diseases;

however, the formulation has been innovated using the original preparation through the continuous implementation of modern technology and made into creams, cataplasms, films, and sponges[2,3].

DFU is a diabetic complication. Its pathogenic causes are often vascular and nerve lesions, resulting in lower limb infection and the formation of foot ulcers[4]. The clinical manifestations are ischemic necrosis or damage to skin tissue, incomplete skin, wound exudation, abscess generation, *etc*. From the perspective of traditional Chinese medicine, DFUs are caused by deficiency of Qi and Yin, weakness of pulse, and blockage of dampness-heat and blood stasis toxin. Traditional chinese medicine also has shown promising effects with regard to safety and renoprotection in some prospective, multicenter, randomized, controlled clinical trial conducted[5]. And studies have found that RHP has a good effect in the treatment of DFUs in traditional Chinese medicine. Shao *et al*[6] found that its combination with antibiotics can quickly reduce the swelling of patients' ulcers to shorten the course of treatment. Liu *et al* [7] treated 40 patients with diabetic skin abscesses with the external application of RHP and found that the rate of effective treatment in the treatment group was higher than the control group. This result shows that RHP has a therapeutic effect on DFU. Zhang[8] treated patients with RHP and Simiao Tongluo decoction and found that this prescription can promote wound healing to promote improvement and play a therapeutic role.

Gas chromatography-mass spectrometry (GC–MS) and ultra-performance liquid chromatography-mass spectrometry (UPLC–MS) are widely used in the separation and identification of complex components, of which GC–MS is mainly used to separate the sample into volatile products in the instrument by pyrolysis of the sample at high temperature, with the advantages of high sensitivity, large information content, high efficiency, and small sample requirements. UPLC–MS technology allows the sample to be separated in the mobile phase after the ionization process through fragment ion mass number analysis and identification. This technology can compensate for the disadvantages of GC–MS, which cannot analyze components with features such as strong polarity, thermal instability, and difficult volatilization; UPLC-MS has the advantages of low detection limit, high automation, wide analysis range, and short analysis time. Network pharmacology research is mainly based on databases and software to obtain important target information for drug treatment of diseases and establish network connections to predict its mechanism of action. Because network pharmacology analysis shows synergy and compatibility with traditional Chinese medicine in the treatment of diseases and the therapeutic principle of syndrome differentiation and treatment, it is widely used in traditional Chinese medicine to explore the mechanism of action in the treatment of diseases from multiple targets. Wound healing is caused by a variety of molecular proteins that affect cells and remodel the tissue. Hematoxylin-eosin (HE) staining electron microscope observation is a more intuitive way to observe the healing of the wound surface. Fibroblasts can be clearly observed to evaluate drug treatment.

Although it has been proven that RHP has a therapeutic effect on DFU, the specific mechanism of action is not clear. In this study, the chemical components of RHP were extracted by supercritical extraction and alcohol extraction and separated and identified by GC–MS and UPLC–MS techniques, respectively, to obtain the active ingredients of the RHP formula, and the target pathway for the treatment of DFU was studied using network pharmacological analysis. In addition, a rat model of DFU was established to verify the therapeutic effect of RHP on wound healing, providing a direction for further clinical research.

## MATERIALS AND METHODS

### Materials

RHP (201202056, Jilin Shuangshi Pharmaceutical Co., Ltd) was purchased from Harbin Shiyitang Chinese Herbal Medicine Co., Ltd. (Harbin, China). Methanol (purity) and acetonitrile (purity) were all obtained from Merck Co., Inc. (Germany). Formic acid (purity) was obtained from West Asia Chemical Technology Co., Ltd. All other chemicals and solvents were of analytical grade.

### Animals and drug administration

Thirty healthy male Sprague Dawley rats (weights, 200 ± 20 g) were purchased from Jinan Pengyue Experimental Animal Breeding Co., Ltd. (Jinan, China) and housed for adaptive feeding for 2 d. The animal facilities and protocols were approved by the Animal Ethics Committee of Heilongjiang University of Chinese Medicine (Heilongjiang, China).

Thirty rats were divided into 3 groups with 10 rats in each group, including the blank, model and RHP groups. The model and RHP groups were injected with streptozotocin/0.1 mol·L$^{-1}$ citrate buffer solution (1/100, g/v). After 72 h, fasting blood glucose was measured with an electronic blood glucose meter (Sannuo Biosensor Co., Ltd, China). The modeling standard was that the random blood glucose level was greater than 12.0 mmol/L, accompanied by the typical symptoms of diabetes mellitus. In the establishment of the ulcer model, the rat hindfoot skin in each group was cut with scissors (the depth of the wound that would reach the fascia). The wound was cleaned before each treatment every day. The wound area was measured on the 5$^{th}$, 7$^{th}$, and 14$^{th}$ days, and the wound-healing rate was calculated. The formula for the healing rate was as follows: Healing rate (%) = (original wound area-unhealed

area)/original wound area × 100%.

After 14 d, the rats were sacrificed, and the skin around the wound was cut into 3 cm × 3 cm areas. The cut tissue was fixed with a 2.5% pentanediol solution and stored at low temperature (-80 °C).

The sample tissues were placed in liquid paraffin, freeze-fixed and sliced. Dewaxing, hydration and dyeing with hematoxylin staining solution and eosin dye solution were performed. The samples were air dried, sealed and observed with transmission electron microscopy (HT7700, Hitachi, Japan).

### Composition analysis of RHP by GC–MS

Supercritical fluid extraction (SFE) equipment (HA220-40-11, Nantong Huaan Supercritical Extraction Co., Ltd, China) was used to extract volatile oil. First, an appropriate amount of RHP sample was crushed and sifted through a 40 μm mesh; the medicinal material was placed into supercritical extraction equipment, and the pressure was boosted to the set parameters for extraction. The pressure of the extraction kettle was 25 MPa, and its temperature was 45 °C. The pressure of the separating kettle was 8 MPa, and its temperature was 60 °C. The pressure of the other separating kettle was 4.5 MPa, and its temperature was 37 °C. The pump frequency of the SFE was 18 Hz, and the flow rate was 60 L/h. After extraction, the materials were removed to obtain the SFE.

GC–MS (5975B, Agilent Technologies, Inc., United States) was used to analyze the chemical composition of the SFE extraction. The prepared SFE extract was vortexed for 2 min, extracted with a solid-phase microextraction needle for 20 min, centrifuged for 20 min, and filtered with a membrane. Each of the samples was injected into GC–MS equipment equipped with an HP-INNOWAX (25 m × 0.20 mm, 0.40 μm) column (Agilent, United States) at 100 °C for 5 min. Then, the temperature was raised to 150 °C at 5 °C/min and then to 280 °C at 30 °C/min. The inlet temperature was 240 °C, and the flow rate of the carrier gas was 1.0 mL/min. The ion source temperature of MS with an EI source was 200 °C, and its transmission line temperature was 250 °C. The bombardment voltage was 70 eV.

### Composition analysis of RHP by UPLC–MS

UPLC–MS (Ultimate 3000LC, Q Exactive HF, Thermo Fisher, United States) was used to analyze the chemical composition of RHP. First, the sample was pulverized, passed through a 40-μm mesh sieve, accurately weighed and placed in a stoppered conical flask. Hydrochloric acid/ethanol solution (1/100, v/v) was accurately added and ultrasonically treated for 40 min. The filtrate was shaken well, filtered and diluted into a 50-mL volumetric flask to obtain a sample solution. The reference substance was precisely weighed and placed in a 10-mL volumetric flask; methanol solution was added, and the solution was diluted to volume after ultrasonic treatment and shaken well to obtain the reference substance solution. Each of the samples was injected into UPLC–MS equipment equipped with a C18 chromatographic (2.1 mm × 100 mm, 1.8 μm) column (Zorbax Eclipse, Agilent, United States) at 30 °C. The flow rate was 0.3 mL/min. The mobile phase was water/formic acid (0.1/100, v/v) (A)/acetonitrile (B). The injection volume was 2 μL.

Mass spectrometry conditions utilized positive and negative modes for UPLC–MS. Electrospray ionization was used in ionization mode with a sheath gas flow rate of 45 arb. The auxiliary gas flow rate was 15 arb. The purge gas flow rate was 1 arb. The electrospray voltage was 3.5 KV. The capillary temperature was 330 °C. The S-Lens RF level was 55%. The scan mode was full scan/dd-MS2 (TopN = 10) with a scanning range of 100-1500 m/z and a resolution of 120000/60000. The collision mode was high energy collision dissociation.

### Building a drug-component-target-disease network relationship graph

Cytoscape (v3.7.2.) is an analysis software that shows the complex corresponding relationship of "drug-component-target-disease" in the form of a network graph. It can conveniently visualize a network relationship, perform network topology analysis, analyze the degree of connection between each node according to the relevant parameters, and thus enable researchers to draw the corresponding conclusions.

### Determining the "Chemical Composition-Target" correspondence

The Traditional Chinese Medicine Systems Pharmacology (TCMSP) database (http://Lsp.nwu.edu.cn/) is a platform for the analysis and study of traditional Chinese medicines in many aspects, and it synthesizes the chemical composition and drug target data of traditional Chinese medicines[9], closely links diseases with targets and components, and explains the mechanism of action of traditional Chinese medicines[10]. The chemical components extracted from ten traditional Chinese medicines of the RHP formula were searched by entering the CAS number of chemical components in the TCMSP database, and the information related to the components could be obtained, of which the "Relatedtarget" column contained the targets corresponding to the component, and the obtained targets were integrated to determine the corresponding relationship between the components and the target.

### Screening targets of RHP

Comparative Toxicogenomics Database (CTD) (http://ctdbase.org/) is a database that brings together detailed information on the intersection between genes, proteins and diseases[11], and the combination

**Table 1 Statistical analysis of wound healing rate at different times**

| Time | 0 d (%) | 3 d (%) | 7 d (%) | 14 d (%) |
|---|---|---|---|---|
| Control group | 0 | 10.41 ± 0.24 | 17.43 ± 0.13 | 33.73 ± 0.28 |
| Experimental group | 0 | 32.78 ± 0.46 | 38.14 ± 0.28 | 53.11 ± 0.07 |
| Homogeneity of variance | – | √ | √ | √ |
| *P* value | – | < 0.05 | < 0.05 | < 0.05 |

of these data with that of their pathways and functions can further elucidate the mechanism of diseases [12]. A component usually corresponds to one or more targets, and information unrelated to the treatment of DFU in the above integrated "component-target" dataset needs to be screened out. In the TCMSP database, the information related to each target in the "Relatedtarget" column above was viewed, the relevant target with the keywords "diabetes-related diseases", "pain" and "bacterial infection" was selected according to the disease type in "Relateddiseases", and its "GenecardID" was recorded. To prevent the limitations of the TCMSP database on the target and disease correspondence and make the study more accurate, the targets without keywords were searched in the CTD database to further determine whether they were related to DFU in the "Diseases" category. Two databases, TCMSP and CTD, were used to screen for and obtain the chemical compositions of targets related to DFU.

### *Molecular docking of ingredients and targets*

DiscoveryStudio (DS v19.1.0) software is a life science molecular simulation software that can be used to establish molecular docking models. Cytoscape was used to visualize the targets and components, analyze the key targets and important components, perform molecular docking, and observe the binding effect of chemical components to target proteins. First, the structural model of the component was downloaded from the TCMSP database; the human protein number corresponding to the target from the UniProt database was queried, and the number from the PDB database was the input to obtain the three-dimensional structural model of the target protein. The component structure and protein structure were opened in DiscoveryStudio software; $H_2O$ and ligand were removed, the protein was hydrogenated, and the relationship between the molecule and the protein was established. In the end, the binding sites can be identified.

### *Pathway enrichment analysis*

The STRING database (https://cn.string-db.org/) and the DAVID database (https://david.ncifcrf.gov) are mainly used to provide information on the individual target genes and proteins or the interaction between multiple histones and to perform GO or KEGG pathway enrichment analysis on them. The STRING database was used to observe the correlation between target proteins of RHP formula herbs, and the DAVID database was used to enrich KEGG pathways for target components and targets to obtain possible pathways for the treatment of DFU.

### *Statistical analyses*

SPSS software (Version 24.0.0, Chicago, IL, United States) was used to analyze the wound-healing rate results of rats at different times, and all data are expressed as the mean ± SD. The differences were considered significant at $P < 0.05$.

## RESULTS

### *In vivo wound healing effect*

During continuous culture for 14 d, the wound areas of the rats on the first, third, seventh, and fourteenth days were recorded, and the cure rate was calculated. The results are shown in Table 1; the difference was significant. The results of the three groups of experiments showed that the cure rate of the RHP group was increased and reached 53.11%, indicating that RHP has a good therapeutic effect on the healing of DFU wounds in rats. The HE staining electron microscope results showed that after 14 d of uninterrupted administration, the ulcer tissues of 10 rats in the model group showed varying degrees of demyelination changes, unlike rats in the blank group, which showed symptoms of neuritis, as shown in Figure 1. In addition, neutrophil infiltration and granulation tissue loosening were observed. The mice treated with powder had good fibroblast function, mature granulation tissue, and restored nerve cells. The thickness of the stratum corneum and the integrity of the epidermis were good, showing a good state of recovery, and intact lymphocytes were observed, but there were a few mast cells. RHP promoted the healing of DFUs in rats by affecting fibroblasts and nerve cells.

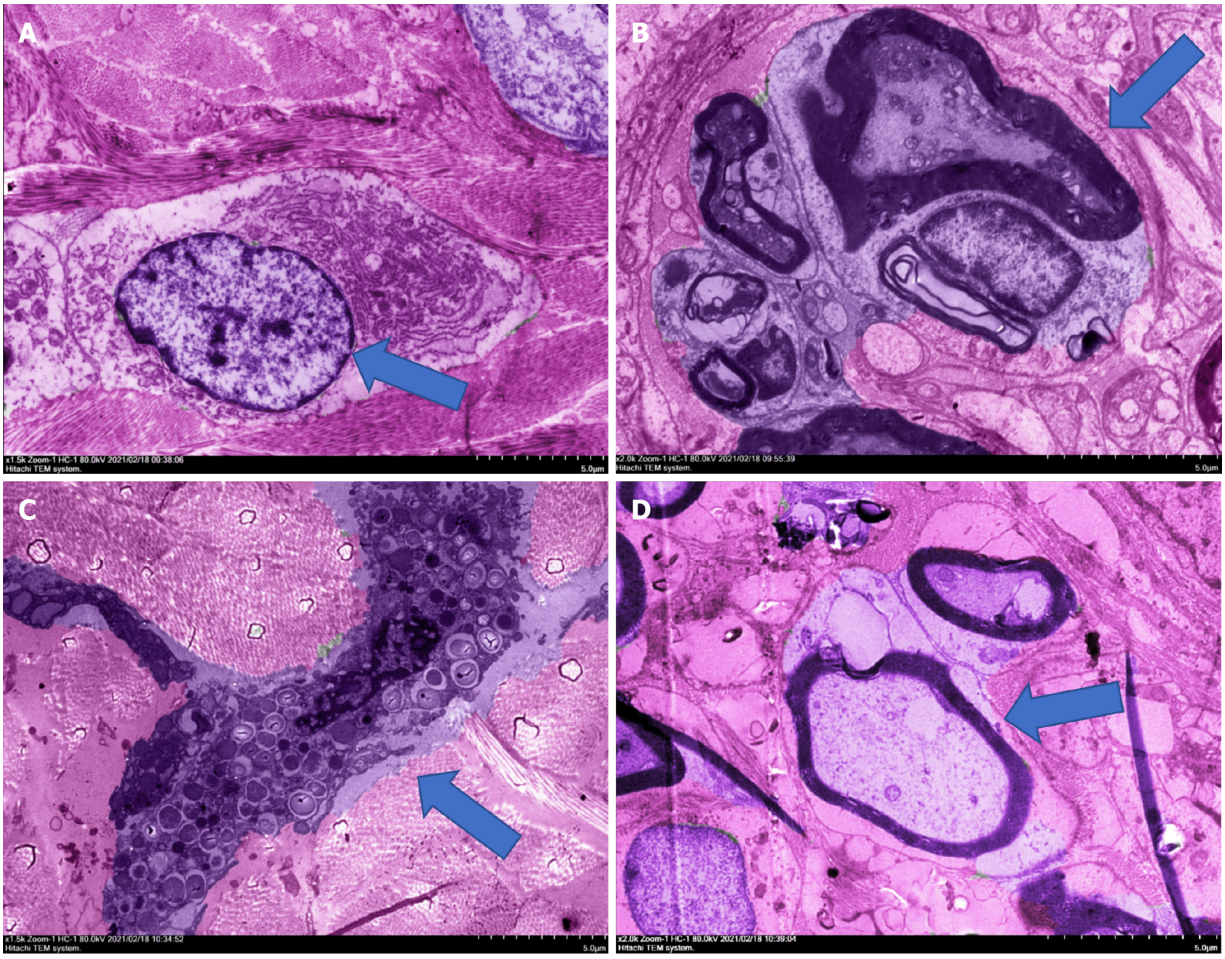


**DOI**: 10.4239/wjd.v13.i8.622 

**Figure 1 Hematoxylin-eosin staining electron micrograph of rat diabetic foot ulcer.** A: The fibroblasts of blank group; B: The neuritis of model group; C: Mast cells of powder group; D: Nerve cells of powder group. The mice treated with powder had good fibroblasts function, mature granulation tissue, and restored nerve cells. The thickness of the stratum corneum and the integrity of the epidermis were good, showing a good state of recovery, and intact lymphocytes would be observed, but there were a few mast cells. Ruyi Jinhuang powder promoted the healing of diabetic foot ulcers in rats by affecting fibroblasts and nerve cells.

### *Composition analysis of RHP by GC–MS*

The GC–MS full spectrum identification results of RHP are shown in Table 2, and a total of 43 components were detected to obtain the total ion flow diagram (Figure 2), which mainly included alcohols, enes, esters, phenols, and other components, accounting for 27.91%, 20.93%, 20.93%, 16.28%, 4.65%, and 9.30% of the total, respectively. Among them, the higher components were ar-turmerone 24.33% (No. 23), tigerone 20.74% (No. 17), agarospirol 13.80% (No. 18), β-eudesmol 9.06% (No. 22), palmitic acid 2.31% (No. 43), and (E)-allylantone 2.23% (No. 29).

### *Composition analysis of RHP by UPLC–MS*

The UPLC–MS full spectrum identification results of RHP are shown in Table 3. A total of 46 components were detected. The main components include flavonoids, organic nitrogens, isopentenol esters, carboxylic acids and their derivatives, benzene and its substituted derivatives, diarylheptans, fatty acyls, anthracyclines and other components, accounting for 23.92%, 15.23%, 10.88%, 8.71%, 6.52%, 6.52%, 6.52%, 4.26% and 17.44% of the total, respectively. The positive and negative ion flow diagrams are shown in Figure 3. Among them, the components with the highest levels were α,α-trehalose (409.04%; No. 6), curcumin (307.20%; No. 37), berberine (232.25%; No. 24), (3R,5R)-1,3,5-trihydroxy-4-{[(2E)-3-(4-hydroxy-3-methoxyphenyl)-2-propenoyl]oxy}cyclohexanecarboxylic acid (201.34%; No. 16), bisdemethoxycurcumin (153.92%; No. 33), genistein (153.83%; No. 39), demethoxycurcumin (151.99%; No. 35), and citricol acid (145.29%; No. 9).

### *Establishment and analysis of the network relationship of "Traditional Chinese Medicine-Ingredients-Target"*

Eighty-nine components were obtained by GC–MS and UPLC–MS. According to the "target-disease" relationship in the database, 43 relevant components for the treatment of DFU were finally screened

**Table 2 Gas chromatography–mass spectrometry full spectrum identification results**

| No. | RT (min) | Relative content (%) | Qualitative | CAS | Name |
|---|---|---|---|---|---|
| 1 | 26.36 | 0.59 | 51.56 | 512-61-8 | (-)-α-Santalene |
| 2 | 27.07 | 0.26 | 25.81 | 87-44-5 | Caryophyllene |
| 3 | 29.71 | 1.86 | 65.77 | 495-60-3 | α-Zingiberene |
| 4 | 29.83 | 0.64 | 14.58 | 495-61-4 | 6-methyl-2-(4-methylcyclohex-3-enyl)hept-1,5-diene |
| 5 | 30.64 | 1.95 | 60.85 | 20307-83-9 | β-Sesquiphellandrene |
| 6 | 30.7 | 1.33 | 80.1 | 644-30-4 | α-Curcumene |
| 7 | 34.21 | 0.38 | 26.47 | 56192-70-2 | (Z)-a-Atlantone |
| 8 | 34.27 | 0.23 | 61.92 | 1139-30-6 | Caryophyllene oxide |
| 9 | 34.36 | 0.30 | 19.52 | 83173-76-6 | 2-Methyl-1-(4-methylphenyl)-3-buten-1-ol |
| 10 | 34.52 | 0.25 | 58.19 | 108549-47-9 | (6Z)-2-Methyl-6-(4-methyl-3-cyclohexen-1-ylidene)-2-hepten-4-one |
| 11 | 35.47 | 0.58 | 29.36 | 639-99-6 | Elemol |
| 12 | 35.78 | 0.28 | 58.71 | 145512-84-1 | Trans-Sesquisabinene hydrate |
| 13 | 36 | 0.37 | 62.02 | 58334-55-7 | Zingiberenol |
| 14 | 36.57 | 0.74 | 86.3 | 6989-21-5 | Atractylon |
| 15 | 36.83 | 0.25 | 12.5 | 82508-14-3 | 2-methyl-6-(4-methylidenecyclohex-2-en-1-yl)hept-2-en-4-one |
| 16 | 37.23 | 0.77 | 22.65 | 1209-71-8 | γ-Eudesmol |
| 17 | 37.41 | 20.74 | 91.81 | 180315-67-7 | Tumerone |
| 18 | 37.67 | 13.80 | 22.04 | 1460-73-7 | Agarospirol |
| 19 | 37.81 | 1.75 | 38 | 112-39-0 | Methyl palmitate |
| 20 | 38.41 | 1.26 | 41.2 | 473-16-5 | a-Eudesmol |
| 21 | 38.48 | 0.72 | 9.97 | 515-20-8 | Costol |
| 22 | 38.65 | 9.06 | 76.48 | 473-15-4 | β-Eudesmol |
| 23 | 39.1 | 24.33 | 97.75 | 532-65-0 | ar-Turmerone |
| 24 | 39.28 | 0.24 | 11.67 | 19888-00-7 | 4,8-Cycloundecadien-1-ol, 6,6,9-trimethyl-2-methylene-, (1R,4E,8E)- |
| 25 | 39.47 | 0.23 | 4.42 | 65646-68-6 | N-(4-hydroxyphenyl)retinamide |
| 26 | 39.64 | 0.39 | 8.22 | 19912-67-5 | (+)-Epicubenol |
| 27 | 39.9 | 0.85 | 49.47 | 30666-87-6 | 2-Methyl-6-(4-methylphenyl)-4-heptanone |
| 28 | 40.16 | 1.05 | 49.07 | 72441-71-5 | (6R,7R)-Bisabolone |
| 29 | 40.53 | 2.23 | 89.2 | 108645-54-1 | (E)-Atlantone |
| 30 | 40.89 | 0.65 | 82.79 | 120681-80-3 | 2-Cyclohexene-1-propanol,g-methyl-4-methylene-a-(2-methyl-1-propen-1-yl) |
| 31 | 41.58 | 0.45 | 75.15 | 112-61-8 | Octadecanoic acid, methyl ester |
| 32 | 41.88 | 1.87 | 16.03 | 112-62-9 | Methyl oleate |
| 33 | 41.98 | 0.65 | 7.88 | 1937-62-8 | trans-octadec-9-enoicacidmethylester |
| 34 | 42.55 | 1.03 | 26.03 | 112-63-0 | methyl linoleate |
| 35 | 43.54 | 0.42 | 42.85 | 301-00-8 | 9,12,15-Octadecatrienoic acid, methyl ester |
| 36 | 43.61 | 0.22 | 4.63 | 29550-55-8 | Teresantalol(7CI) |
| 37 | 44.58 | 0.24 | 88.5 | 69301-27-5 | 2-(1,5-Dimethyl-4-Hexenyl)-5-Methyl-Phenol |
| 38 | 43.85 | 0.84 | 6.23 | 38142-57-3 | 2-Methyl-6-(p-tolyl)hept-2-en-4-ol |
| 39 | 45.01 | 1.11 | 28.14 | 3218-36-8 | 4-Biphenylcarboxaldehyde |
| 40 | 46.86 | 0.84 | 75.64 | 4666-84-6 | Proximadiol |
| 41 | 47.75 | 0.46 | 98.07 | 949081-10-1 | (S)-3-Methyl-6-((S)-6-methyl-4-oxohept-5-en-2-yl)cyclohex-2-enone |

| | | | | | |
|---|---|---|---|---|---|
| 42 | 48.71 | 0.24 | 9.54 | 2566-90-7 | Methyl 4,7,10,13,16,19-cis-docosahexanenoate |
| 43 | 51.08 | 2.31% | 83.12 | 1957-10-3 | Palmitic acid |

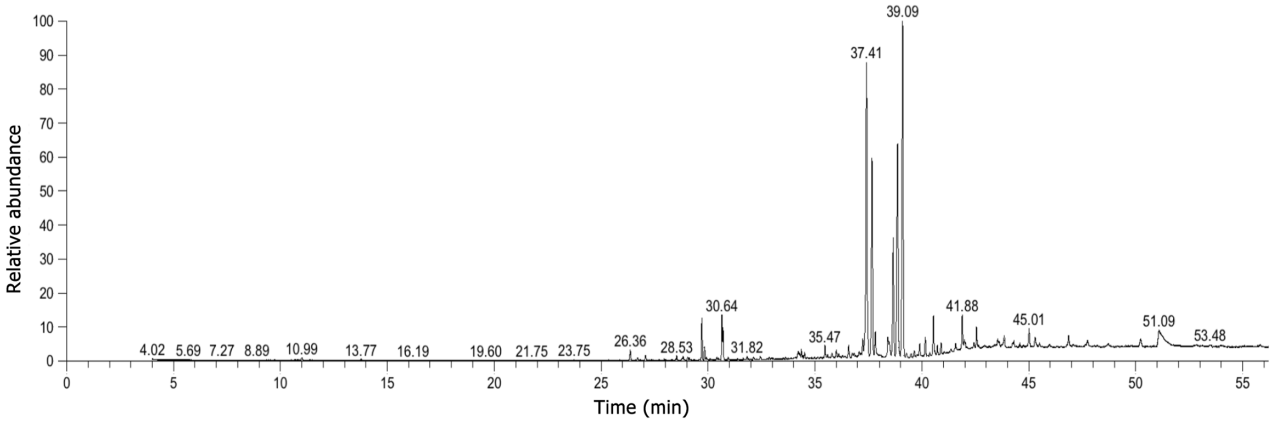


**DOI**: 10.4239/wjd.v13.i8.622 **Copyright** ©The Author(s) 2022.

**Figure 2 The total ion flow diagram of gas chromatography–mass spectrometry.** Among them, the higher components were ar-turmerone 24.33%, tumerone 20.74%, agarospirol 13.80%, β-eudesmol 9.06%, palmitic acid 2.31%, (E) atlantone 2.23%, β-quadruphellandrene 1.95%, methyloleate 1.87%, α-zingiberene 1.86%, and methylmitate 1.75%.

from the ten medicines. There were 36 related targets. The results are shown in Table 4. Cytoscape software was used to visualize the network relationship of "TCM-Ingredient-Target", which was constructed by the parameters of "Degree", "Betweenness" and "Closeness" of each node, as shown in Figure 4. The important medicinal materials of RHP for the treatment of DFU are *turmeric, Magnolia officinalis*, and *rhubarb*, and the important components are luteolin, naringin, demethoxycurcumin, gallic acid, methyl linoleate, caryophyllene, arylcurcumin, methyl palmitate, berberine and rheic acid. The important targets are posttranscriptional silencing (PTGS2), muscarinic acetylcholine receptor M2 (CHRM2), Dipeptidyl peptidase 4, topoisomerase II alpha (TOP2A), retinoic X receptor alpha (RXRA), Protein tyrosine phosphatase nonreceptor type 1, tumor necrosis factor (TNF), interleukin 6 (IL-6), *etc.*

### *Analysis of the docking results of important components and key target molecules*

Molecular docking was performed between important components of luteolin, methyl palmitate, ar-turmeric, methyl linoleate, palmitic acid, demethoxycurcumin, and naringin and the key targets PTGS2, TOP2A, CHRM2, and RXRA. The results are shown in Table 5, in which LibDockScore indicates the docking effect, and the value indicates the docking effect. Seven components (luteolin, methyl palmitate, ar-turmeric, methyl linoleate, palmitic acid, demethoxycurcumin and naringin) had a large LibDockScore, indicating that the binding effect between these components and key targets was good. The component docking conformations shown in Figure 5 indicate the following: The complex naringin-PTGS2 was stabilized by five conventional hydrogen bonds, eight carbon-hydrogen bonds, and two bonds to the alkyl with residues including GLY, ANS, ARG, PHE, ASN, HIS, GLY, GLN, LEU; the complex methyl linoleate-RXRA was stabilized by three carbon-hydrogen bonds, two Pi bonds to the alkyl with residues including DA and DG; the complex luteolin-TOP2A was stabilized by four conventional hydrogen bonds, two carbon-hydrogen bonds, two Pi bonds to the alkyl, six Pi bonds to the benzene ring with residues including LYS, GLU, SER, and ASP; the complex naringin-TOP2A was stabilized by three conventional hydrogen bonds, four carbon-hydrogen bonds, one Pi bond to the alkyl, four Pi bonds to the benzene ring with residues including ASP, ARG, ASN, and LYS; the complex methyl palmitate-PTGS2 was stabilized by two conventional hydrogen bonds, one Pi bond to the alkyl with residues including VAL, ASN, and TRP; the complex ar-turmeric-CHRM2 was stabilized by nine Pi bonds to the alkyl, two Pi bonds to the benzene ring and Van der Waals interactions with residues including PHE, LYS, ILE, VAL, LEU, ASP, ARG, ASN, and THR; the complex methyl linoleate-PTGS2 two carbon-hydrogen bonds, one Pi bond and one bond to the alkyl with residues including VAL, ASN, ILE, and TRP; the complex ar-turmeric-PTGS2 was stabilized by one conventional hydrogen bond, one Pi bond and three bonds to the alkyl, two Pi bonds to the benzene ring with residues including GLN, PHE, VAL, PRO, and ASN; the complex palmitic acid-PTGS2 was stabilized by two conventional hydrogen bonds with residues including VAL and GLY; the complex demethoxycurcumin-PTGS2 was stabilized by four conventional hydrogen bonds, one carbon-hydrogen bond, three Pi bonds to the benzene ring with residues including GLY, VAL, ASN, and PHE.

**Table 3 Ultra-performance liquid chromatography full spectrum identification results**

| No. | Name | CAS | Molecular weight | RT (min) | Relative concentration (μg/mL) |
|---|---|---|---|---|---|
| 1 | DL-Arginine | 7200-25-1 | 174.11175 | 0.783 | 24.44253696 |
| 2 | Nitrosobis(2-oxopropyl)amine | 60599-38-4 | 158.06914 | 0.817 | 15.74503993 |
| 3 | Gluconic acid | 526-95-4 | 196.05765 | 0.821 | 82.48616363 |
| 4 | D-(+)-Proline | 344-25-2 | 115.06357 | 0.846 | 15.35704499 |
| 5 | Cabotegravir | 1051375-10-0 | 405.11182 | 0.847 | 20.08010135 |
| 6 | α,α-Trehalose | 99-20-7 | 342.11623 | 0.847 | 409.0449144 |
| 7 | D-(-)-Quinic acid | 77-95-2 | 192.06275 | 0.85 | 56.2670819 |
| 8 | Isocitric acid | 320-77-4 | 192.02637 | 0.939 | 63.29259087 |
| 9 | Citric acid | 77-92-9 | 192.02637 | 1.169 | 145.2856943 |
| 10 | Gallic acid | 149-91-7 | 170.02078 | 1.899 | 23.57871448 |
| 11 | Chlorogenic acid | 327-97-9 | 354.09527 | 5.332 | 44.58986172 |
| 12 | Catechin | 88191-48-4 | 290.07917 | 5.431 | 98.07463825 |
| 13 | methyl chlorogenate | 123483-19-2 | 368.11081 | 5.501 | 18.15074983 |
| 14 | 6-Acetylcodeine | 6703-27-1 | 341.16237 | 5.886 | 12.3548527 |
| 15 | 2-(3,4-Dihydroxyphenyl)ethyl 3-O-(6-deoxy-β-L-mannopyranosyl)-6-O-[(2E)-3-(3,4-dihydroxyphenyl)-2-propenoyl]-β-D-glucopyranoside | 61303-13-7 | 624.20617 | 6.092 | 20.78761602 |
| 16 | (3R,5R)-1,3,5-Trihydroxy-4-{[(2E)-3-(4-hydroxy-3-methoxyphenyl)-2-propenoyl]oxy}cyclohexanecarboxylic acid | 2613-86-7 | 368.11084 | 6.196 | 201.3429867 |
| 17 | Emodin-8-Beta-D-Glucoside | 23313-21-5 | 432.10571 | 6.579 | 7.280885459 |
| 18 | 2-[4-[3-[3,4-dihydroxy-4-(hydroxymethyl)oxolan-2-yl]oxy-4,5-dihydroxy-6-(hydroxymethyl)oxan-2-yl]oxyphenyl]-7-hydroxy-2,3-dihydrochromen-4-one | 74639-14-8 | 550.16902 | 6.625 | 13.98565399 |
| 19 | Baicalin | 21967-41-9 | 446.0852 | 6.663 | 16.85569046 |
| 20 | Liquiritin | 551-15-5 | 418.12676 | 6.737 | 22.91985259 |
| 21 | Naringin | 10236-47-2 | 580.17964 | 6.959 | 26.36327029 |
| 22 | Hesperidin | 520-26-3 | 610.19038 | 7.191 | 85.82076776 |
| 23 | Azelaic acid | 123-99-9 | 188.1042 | 7.548 | 4.773123466 |
| 24 | Berberine | 2086-83-1 | 335.11525 | 8.242 | 232.2489146 |
| 25 | isosakuranetin-7-O-rutinoside | 14259-47-3 | 594.19556 | 8.493 | 4.34803523 |
| 26 | Tinnevellin glucoside | 80358-06-1 | 408.14228 | 8.786 | 13.59498227 |
| 27 | Daidzein | 486-66-8 | 254.05778 | 9.009 | 13.05981793 |
| 28 | Chrysophanol 8-O-β-D-glucoside | 13241-28-6 | 416.11099 | 9.01 | 17.88080565 |
| 29 | Licoricesaponin G2 | 118441-84-2 | 838.39998 | 9.824 | 7.195669531 |
| 30 | Luteolin | 491-70-3 | 286.04776 | 9.909 | 1.034661042 |
| 31 | (15Z)-9,12,13-Trihydroxy-15-octadecenoic acid | 95341-44-9 | 330.24071 | 9.938 | 19.41925634 |

| | | | | | |
|---|---|---|---|---|---|
| 32 | Rheic acid | 478-43-3 | 284.03211 | 11.029 | 81.8044913 |
| 33 | Bisdemethoxycurcumin | 24939-16-0 | 308.10496 | 11.328 | 153.9247824 |
| 34 | 6-Hydroxy-2-naphthoic acid | 16712-64-4 | 188.04652 | 11.328 | 7.047135466 |
| 35 | Demethoxycurcumin | 22608-11-3 | 338.11567 | 11.473 | 151.9906609 |
| 36 | 5,7-dihydroxy-2-(4-hydroxy-3-methoxyphenyl)-6-(3-methylbut-2-enyl)-2,3-dihydro-chromen-4-one | 76735-58-5 | 370.14168 | 11.541 | 55.08087646 |
| 37 | Curcumin | 458-37-7 | 368.12606 | 11.619 | 307.1972754 |
| 38 | Isoimperatorin | 482-45-1 | 270.08918 | 11.847 | 1.025466018 |
| 39 | Genistein | 446-72-0 | 270.05279 | 12.256 | 153.8276373 |
| 40 | (+/-)9-HODE | 98524-19-7 | 296.23511 | 13.146 | 23.43829567 |
| 41 | (+)-ar-Turmerone | 532-65-0 | 216.15135 | 13.605 | 23.84749189 |
| 42 | Indane | 496-11-7 | 118.07843 | 13.605 | 27.63249372 |
| 43 | Prespatane | 100387-71-8 | 204.18777 | 13.956 | 2.010509748 |
| 44 | (+)-Nootkatone | 4674-50-4 | 218.16696 | 14.497 | 16.6606139 |
| 45 | Aristolone | 6831-17-0 | 218.16696 | 14.588 | 45.88543598 |
| 46 | 2,2'-Methylenebis(4-methyl-6-tert-butylphenol) | 119-47-1 | 340.24015 | 16.788 | 25.70628216 |

RT: Radiotherapy.

### *Analysis of KEGG pathway enrichment results*

The interaction between each target protein was preliminarily obtained by entering the target protein into the STRING database, as shown in Figure 6. Among the 36 targets, except for CHRM2, CHRM4, PCYT1A and Sodium voltage-gated channel alpha subunit 5, the remaining 32 target proteins are closely related to each other and may participate in multiple pathways. The target list was uploaded to the DAVID database to establish the "pathway-target" link. A total of 27 pathways related to DFU treatment were retrieved. The number of targets contained in each pathway is shown in Figure 7A. Cytoscape was used to construct the "pathway-target" network relationship diagram, which is shown in Figure 7B; the "pathway-target" relationship is shown in Figure 7C. Correspondence between channel categories is shown in Figure 7D. Most of the 27 pathway diagrams belong to the immune system and participate in the processes of inflammatory and infectious diseases, which demonstrate signal transduction effects. This finding shows that RHP can affect the body's immune system, regulate inflammation through signal transduction, and exert curative effects in DFU. Further analysis of the literature shows that RHP is mainly related to the phosphoinositide 3-kinase (PI3K)-protein kinase B (Akt) signaling pathway, neuroactive ligand–receptor interaction and the forkhead box O (FoxO) signaling pathway in the treatment of DFU.

We established the network relationship between the three pathways of the PI3K-Akt signaling pathway, neuroactive ligand–receptor interaction and FoxO signaling pathway and the target and chemical components and analyzed the topological parameters of each node. The network diagram (Figure 8) showed that CHRM2 and RXRA are the common targets of the three pathways.

### *The prediction of anti-DFU mechanism*

According to the literature, wound healing mainly involves the three processes of hemostasis and inflammation, proliferation, and remodeling. The target pathways involved are diverse and complex, as shown in Figure 9. RHP can act on leukocytes by regulating IL-6 and TNF, regulating the inflammatory response, and then participating in hemostasis to participate in inflammation and remodeling stages. RHP can also affect platelets, macrophages and fibroblasts by acting on the PI3K-Akt pathway to promote angiogenesis participation in the proliferation stage and facilitate wound healing in DFUs.

Further analysis of the effects of the three pathways in the human body found that if the PI3K-Akt signaling pathway is inhibited in diabetic neurons, neuronal apoptosis is increased, and diabetic neuropathic pain is induced; thus, activating this pathway can alleviate painful diabetic peripheral neuropathy. The abnormal expression or loss of genes related to the neuroactive ligand–receptor interaction pathway can cause neuropathy, such as with the downregulation of glial gene expression, which impairs nerve impulse conduction and increases the potential nerve involvement of systemic

**Table 4 Ruyi Jinhuang powder "Chinese medicine-ingredients-target" correspondence**

| CAS | Name | GenecardID | Attribution |
|---|---|---|---|
| 512-61-8 | (-)-α-Santalene | PTGS2, CHRM2 | JH |
| 87-44-5 | Caryophyllene | PTGS2, CHRM2 | BZ, JH, CZ, ZHP, TNX |
| 495-60-3 | α-Zingiberene | PTGS2, DPP4 | JH |
| 20307-83-9 | β-Sesquiphellandrene | PTGS2 | JH |
| 644-30-4 | α-Curcumene | PTGS2, TOP2A, DPP4 | JH |
| 1139-30-6 | Caryophyllene oxide | CHRM2, DPP4 | ZHP, TNX |
| 639-99-6 | Elemol | CHRM2 | ZHP, JH |
| 58334-55-7 | Zingiberenol | CHRM2 | JH |
| 6989-21-5 | Atractylon | SCN5A, CHRM4, HTR2A, CHRM2, OPRM1 | CZ |
| 82508-14-3 | 2-methyl-6-(4-methylidenecyclohex-2-en-1-yl)hept-2-en-4-one | PTGS2, CHRM2 | JH, ZHP, CZ |
| 112-39-0 | Methyl palmitate | PTGS2, IL-10, TNF, IL-6 | JH, ZHP, BZ, HB, THF |
| 473-15-4 | beta-Eudesmol | CHRM2 | ZHP, JH, CZ |
| 532-65-0 | (6S)-2-methyl-6-(4-methylphenyl)hept-2-en-4-one | DPP4, PTGS2, CHRM2x, ampC | JH |
| 112-62-9 | Methyl oleate | RXRA | ZHP, THF |
| 1937-62-8 | trans-octadec-9-enoicacidmethylester | RXRA | ZHP, THF |
| 112-63-0 | methyl linoleate | PTGS2, RXRA | BZ, THF, ZHP, TNX |
| 301-00-8 | 9,12,15-Octadecatrienoic acid, methyl ester, (Z,Z,Z)- | PTGS2, RXRA | THF |
| 38142-57-3 | 2-Methyl-6-(p-tolyl)hept-2-en-4-ol | PTGS2, CHRM2, DPP4, ampC, RXRA | THF, ZHP, TNX |
| 1957—10—3 | Palmitic acid | PTGS2, IL-10, TNF, PCYT1A | DH, ZHP, THF |
| 149-91-7 | Gallic acid | PTGS2, PTPN1, TOP2A | DH, TNX, CP, GC, JH |
| 23313-21-5 | Emodin-8-Beta-D-Glucoside | TOP2A | DH |
| 458-37-7 | Curcumin | PTGS2, PTPN1 | JH |
| 22608-11-3 | Demethoxycurcumin | PTGS2, PTPN1, AKR1B1, ABCB1, SCN5A | JH |
| 520-26-3 | Hesperidin | PTGS2 | CP |
| 14259-47-3 | isosakuranetin-7-O-rutinoside | TOP2A | CP |
| 10236-47-2 | Naringin | TOP2A, CDKN1A, TNF, RASGRF2, RAF, PTGS2, ampC, MTTP, APOB, mvaA, PPARA | CP, GC |
| 21967-41-9 | Baicalin | PTPN1, TOP2A | DH |
| 88191-48-4 | Catechin | CHRM2 | DH, CP |
| 491-70-3 | Luteolin | PTGS2, DPP4, EGFR, IL10, CDK4, TNF, IL6, NFKBIA, psdA1, IL2, TOP2A, SLC2A4, INSR, MET | CP, ZHP |
| 551-15-5 | Liquiritin | PTGS2 | GC |
| 478-43-3 | Rheic acid | PTGS2, AKR1B1 | DH |
| 2086-83-1 | Berberine | PTGS2, RXRA | HB |
| 77-92-9 | Citric acid | PTGS2, AKR1B1, GRIN2A, GRIA2, PTPN1 | DH |
| 320-77-4 | Isocitric acid | PTGS2 | DH |
| 7200-25-1 | DL-Arginine | PTGS2 | THF |

| | | | |
|---|---|---|---|
| 446-72-0 | Genistein | PTGS2, EGFR, TNF, SELE, IL8 | GC |
| 482-45-1 | Isoimperatorin | PTGS2 | BZ |
| 486-66-8 | Daidzein | PTGS2, RXRA | GC |
| 6831-17-0 | Aristolone | CHRM2, PTGS2 | BZ |
| 532-65-0 | (+) -ar-Turmerone | PTGS2, RXRA, CHRM2, ampC, DPP4 | JH |
| 327-97-9 | Chlorogenic acid | PTGS2 | HB |
| 77-95-2 | D-(-)-Quinic acid | PTGS2 | HB |
| 1460-73-7 | Agarospirol | CHRM2 | ZHP |

TNF: Tumor necrosis factor; IL: Interleukin; PTGS2: Posttranscriptional silencing; TOP2A: Topoisomerase II alpha; CHRM2: Muscarinic acetylcholine receptor M2; RXRA: Retinoic X receptor alpha; DPP4: Dipeptidyl peptidase 4; SCN5A: Sodium voltage-gated channel alpha subunit 5; HTR2A: 5-hydroxytryptamine (serotonin) receptor 2A; OPRM1: Opioid Receptor Mu 1; EGFR: Epidermal Growth Factor Recepto; PTPN1: Protein tyrosine phosphatase nonreceptor type 1; THF: Trichosanthin (Tian Hua); DH: Rhubarb (Da Huang); HB: Phellodendron (Huang Bai); JH: Turmeric (Jiang Huang); BZ: Angelica dahurica (Bai Zhi); TNX: Arisaema (Tian Nan Xing); CZ: Atractylodes lancea (Cang Zhu); HP: Magnolia officinalis (Hou Po); CP: Pericarpium Citri Reticulatae (Chen Pi); GC: Glycyrrhiza uralensis (Gan Cao).

**Table 5 Docking parameters of chemical components and target protein molecules**

| Name | Target | LibDockScore |
|---|---|---|
| Luteolin | TOP2A | 104.333 |
| Methyl palmitate | PTGS2 | 114.221 |
| ar-Turmeric | PTGS2 | 91.0625 |
| | CHRM2 | 88.3765 |
| Methyl Linoleate | RXRA | 138.583 |
| | PTGS2 | 130.838 |
| Palmitic acid | PTGS2 | 114.349 |
| Demethoxycurcumin | PTGS2 | 135.479 |
| Naringin | TOP2A | 141.197 |
| | PTGS2 | 164.305 |

PTGS2: Posttranscriptional silencing; TOP2A: Topoisomerase II alpha; CHRM2: Muscarinic acetylcholine receptor M2; RXRA: Retinoic X receptor alpha.

diseases. The link between the FoxO signaling pathway and diabetes is that type II diabetes mellitus causes abnormal tissue signaling due to hyperglycemia or insulin resistance. The identified important targets, such as IL-6 and TNF, participate in the abovementioned pathways and play a role in hemostasis and tissue remodeling so that the DFU wound can heal. The mechanism of action is shown in Figure 10.

## DISCUSSION

The results of the three groups of experiments showed indicated that RHP has a good therapeutic effect on the healing of DFU wounds in rats. The HE staining electron microscopy results showed neutrophil infiltration and granulation tissue loosening in the model group and blank group. The fibroblasts of the RHP group had good function, the granulation tissue was mature, and nerve cells were restored. The thickness of the stratum corneum and the integrity of the epidermis were good, showing a good state of recovery, and intact lymphocytes could be observed, but there were a few mast cells. Thus, RHP promoted the healing of DFUs in rats by affecting fibroblasts and nerve cells.

In this study, GC–MS and UPLC–MS were used to collect and identify the chemical components of RHP. Eighty-nine compounds were detected and analyzed, including flavonoids, terpenes, and coumarins. The components obtained by GC–MS are mainly volatile substances, and the components obtained by UPLC–MS are mostly high boiling point, nonvolatile, high molecular weight substances. The network pharmacology analysis of these compounds shows that RHP plays a role in the treatment

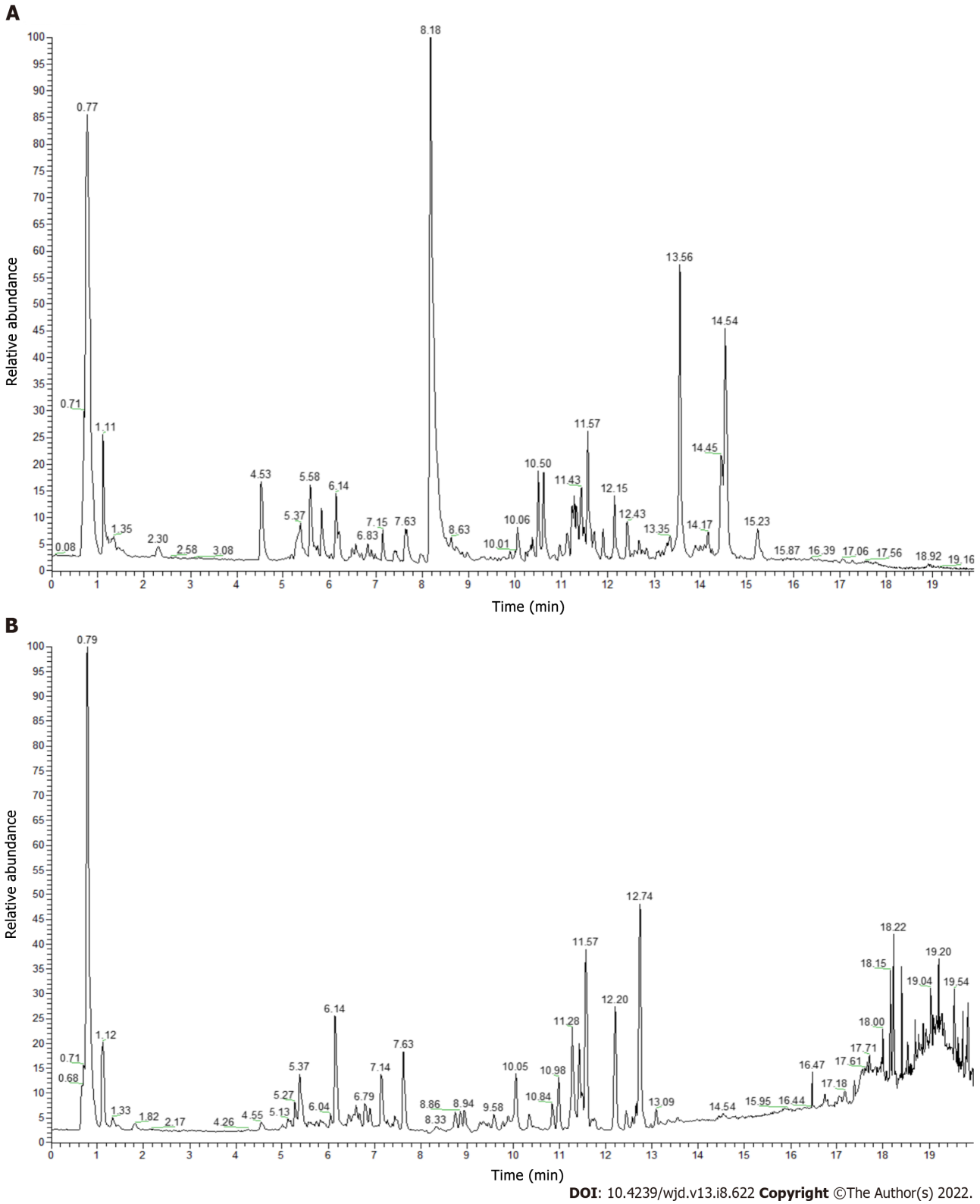


**DOI**: 10.4239/wjd.v13.i8.622 **Copyright** ©The Author(s) 2022.

**Figure 3 Ultra-performance liquid chromatography ion flow diagram of Ruyi Jinhuang powder.** A: Positive ion flow diagram; B: Negative ion flow diagram. Among them, the components with high levels were α,α-trehalose 409.04% (No. 6), curcumin 307.20% (No. 37), berberine 232.25% (No. 24), (3R,5R)-1,3,5-trihydroxy-4-{[(2E)-3-(4-hydroxy-3-methoxyphenyl)-2-propenoyl]oxy}cyclohexanecarboxylic acid 201.34% (No. 16), bisdemethoxycurcumin 153.92% (No. 33), genistein 153.83% (No. 39), demethoxycurcumin 151.99% (No. 35), and citricol acid 145.29% (No. 9).

of DFUs through multiple targets and channels. However, the manner in which specific components are combined with target proteins needs to be further explored.

DFU is one of the main complications of diabetes. Current studies have found that its main causes are neuropathy, vascular disease and impaired immune function[13,14]. The specific pathogenesis is that when persistent hyperglycemia occurs, nerve cells accumulate a large number of toxic components,

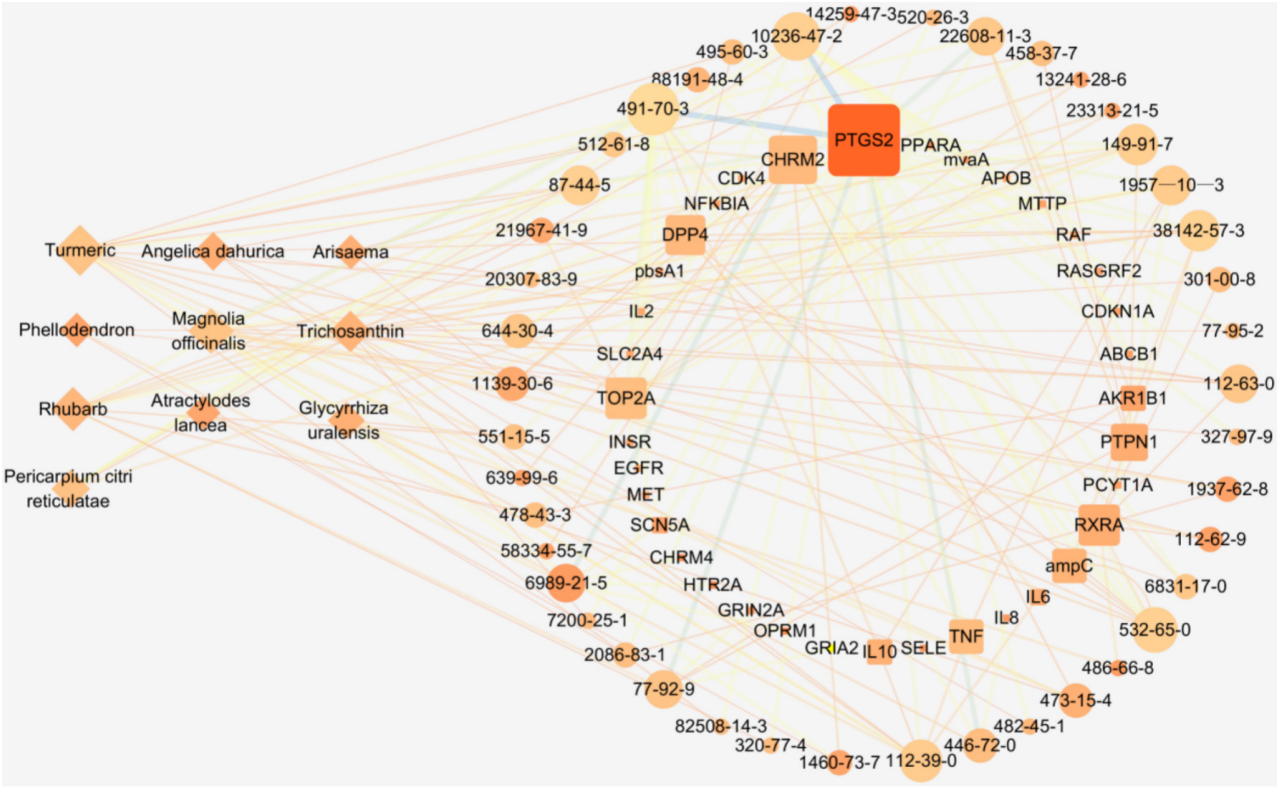


**DOI**: 10.4239/wjd.v13.i8.622 

**Figure 4 The "traditional Chinese medicine-ingredient-target" network of Ruyi Jinhuang powder topology diagram.** There are a total of 89 nodes and 186 edges; diamonds represent ten herbs of Ruyi Jinhuang powder, circles represent 43 related chemical components (represented in the form of CAS number), squares represent 36 target targets (represented in the form of GenecardID), nodes indicate that the greater Degree value, the darker color indicates the greater Closness value, and the thicker lines indicate the greater Betweenness value.

damage to endothelial cell function occurs, vascular tension is decreased, and nerve ischemia occurs; thus, nerve and vascular lesions develop. In addition, persistent hyperglycemia affects the inflammatory response of the wound by acting on cells and the immune system, and the wound is persistently infected and difficult to heal[15,16].

The active ingredients were extracted from the ten herbs of RHP, and network pharmacological analysis of "herb-component-target pathway-disease" was performed to identify three key pathways: The PI3K-Akt signaling pathway; neuroactivated-receptor interactions; and the FoxO signaling pathway. These pathways are important targets for the treatment of DFU. Studies have found that RXRA has a negative regulatory effect on glucose-stimulated insulin secretion[17], while CHRM2 mainly plays a role in the central nervous system and peripheral nervous system and can activate endothelial cell NO lyase to relax vascular smooth muscle[18,19], which is a major cause of foot ulcers caused by diabetic vascular disease and is a key target for the treatment of vascular disease[20]. The mechanism of the PI3K-Akt signaling pathway in the treatment of DFU is reflected in the following two aspects. On the one hand, insulin initiates this signaling pathway by upregulating PI3K expression with Akt molecules and inhibits FoxO1 expression, thereby allowing normal glucose uptake by cells and improving abnormal lipid metabolism[21-23]. On the other hand, if the PI3K-Akt signaling pathway is inhibited in diabetic neurons, neuronal apoptosis is increased, and diabetic neuropathic pain is induced; thus, activation of this pathway can relieve painful diabetic peripheral neuropathy[24]. In addition, diabetic patients have difficulty healing repeated wound infections due to a prolonged wound inflammatory response due to metabolic disorders, and the PI3K-Akt signaling pathway can promote the expression of hypoxia-inducible Factor 1, an important factor in wound healing, to accelerate wound cell proliferation to promote healing[25]. The neuroligand-interreceptor interaction pathway is a collection of intracellular and extracellular related receptor ligands, and abnormal expression or deletion of related genes in this pathway can cause neuropathic lesions; for example, downregulation of Glral gene expression impairs nerve impulse conduction and increases the potential incidence of neurological diseases[26,27]. The link between the FoxO signaling pathway and diabetes is that type 2 diabetes induces skeletal muscle atrophy due to abnormal tissue signaling and protein disorders caused by hyperglycemia or insulin resistance, and insulin phosphorylates mediators of the FoxO signaling pathway and inhibits autophagy-related gene expression. Luteolin can reduce neuropathic pain by decreasing FoxO1 acetylation, regulating this pathway, and inhibiting the expression of inflammation- and pain-related genes[28]. In addition to these three pathways, the PI3K-Akt signaling pathway,

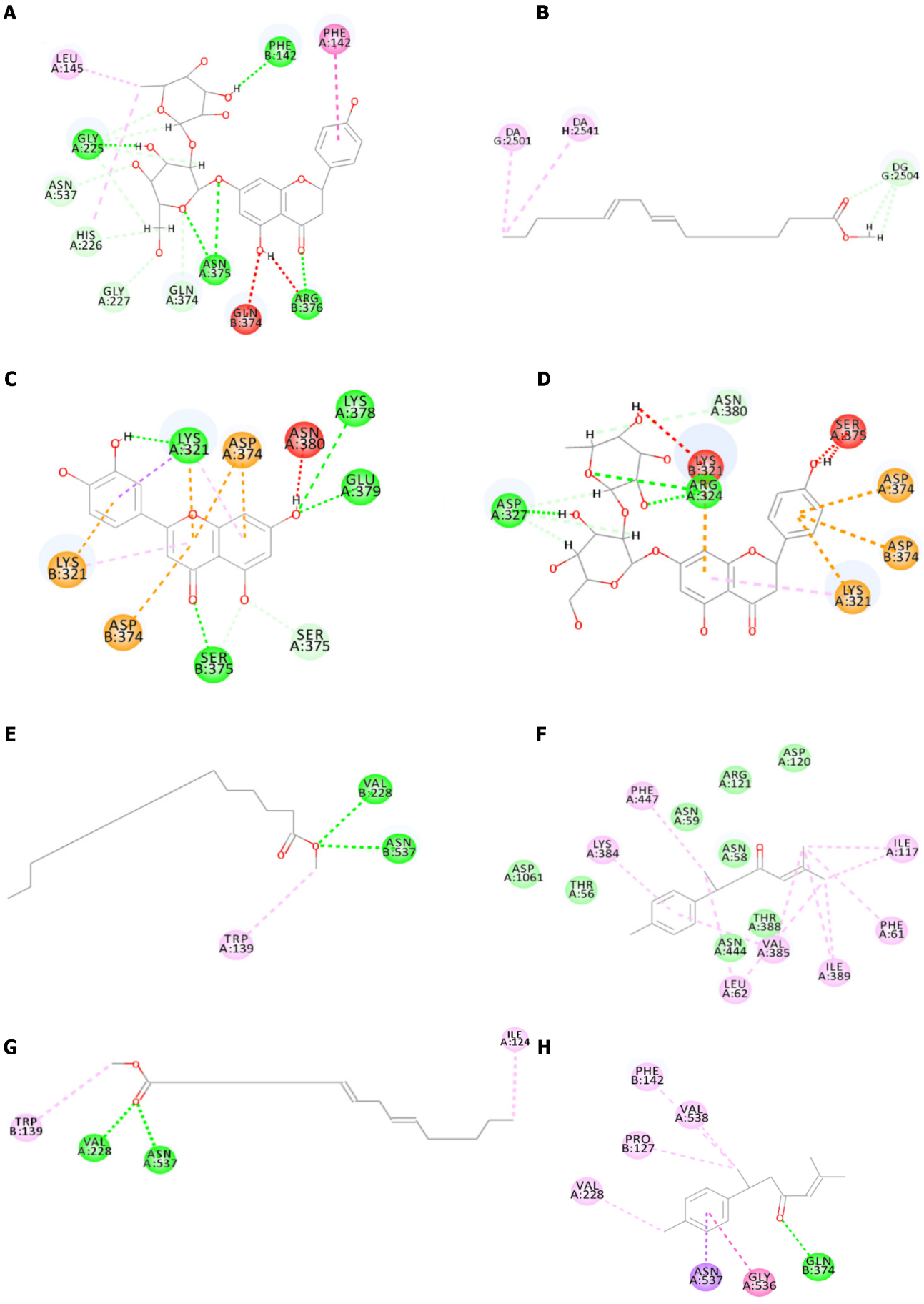
A
LEU A:145
PHE B:142
PHE A:142
GLY A:225
ASN A:537
HIS A:226
ASN A:375
GLY A:227
GLN A:374
GLN B:374
ARG B:376
B
DA G:2501
DA H:2541
DG G:2504
C
LYS A:378
LYS A:321
ASP A:374
ASN A:380
GLU A:379
LYS B:321
ASP B:374
SER B:375
SER A:375
D
ASN A:380
SER A:375
LYS B:321
ARG A:324
ASP A:374
ASP A:327
ASP B:374
LYS A:321
E
VAL B:228
ASN B:537
TRP A:139
F
ASP A:120
ARG A:121
PHE A:447
ASN A:59
LYS A:384
ASN A:58
ILE A:117
ASP A:1061
THR A:56
THR A:388
PHE A:61
ASN A:444
VAL A:385
ILE A:389
LEU A:62
G
ILE A:124
TRP B:139
VAL A:228
ASN A:537
H
PHE B:142
VAL A:538
PRO B:127
VAL A:228
GLN B:374
ASN A:537
GLY A:536

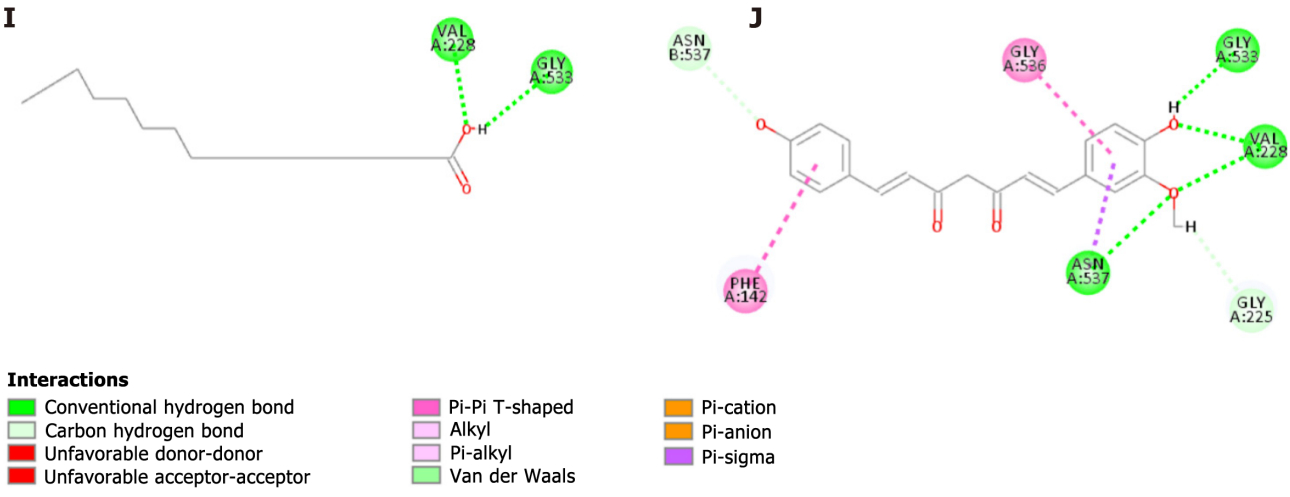


**DOI**: 10.4239/wjd.v13.i8.622 **Copyright** ©The Author(s) 2022.

**Figure 5 The virtual docking of bioactive ingredients from Ruyi Jinhuang powder for diabetic foot ulcer targets.** A and D: The virtual docking of naringin with post-transcriptionalgenesilencing (PTGS2) and Topoisomerase II alpha (TOP2A); B and G: The virtual docking of methyl linoleate with Retinoid X Receptor alpha and PTGS2; C: The docking of Luteolin and TOP2A; E: The docking of Methyl palmitate and PTGS2; F and H: The virtual docking of ar-Turmeric with Muscarinic Acetylcholine receptor M2 and PTGS2; I: The virtual docking of palmitic acid and PTGS2. J represents the virtual docking of demethoxycurcumin and PTGS2.

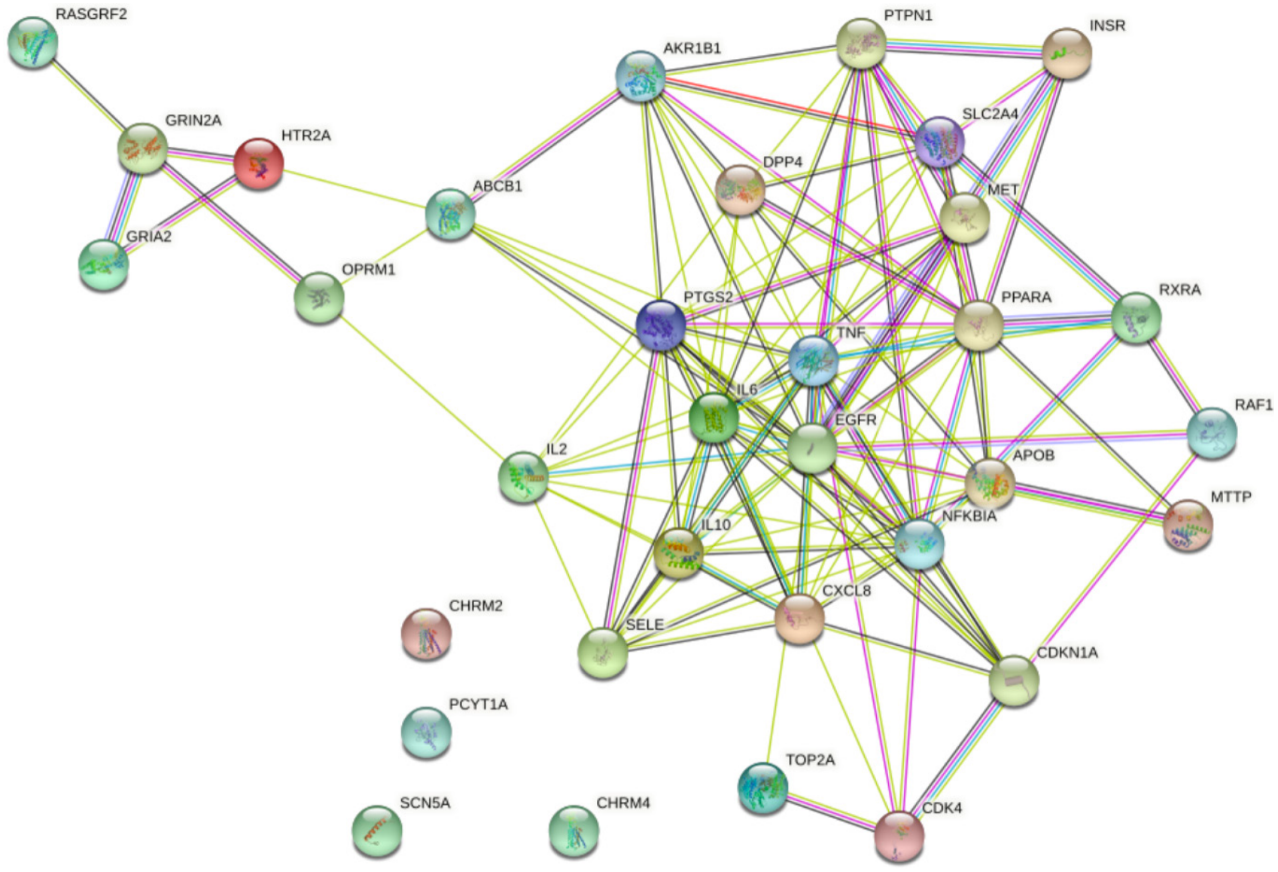


**DOI**: 10.4239/wjd.v13.i8.622 **Copyright** ©The Author(s) 2022.

**Figure 6 Interaction diagram of target proteins.** The edges with different colors represent different association relationships. Among the 36 targets, except for Muscarinic Acetylcholine receptor M2 (CHRM2), CHRM4, Choline-phosphate cytidylyltransferase A and Sodium channel protein type 5 subunit alpha, the remaining 32 target proteins are closely related to each other and may participate in multiple pathways.

neuroactivated-receptor interactions, and the FoxO signaling pathway, the network topological properties of the human T-cell leukemia virus-infection signaling pathway were also found to be prominent in the RHP network pharmacology analysis; however, there is no specific research result on

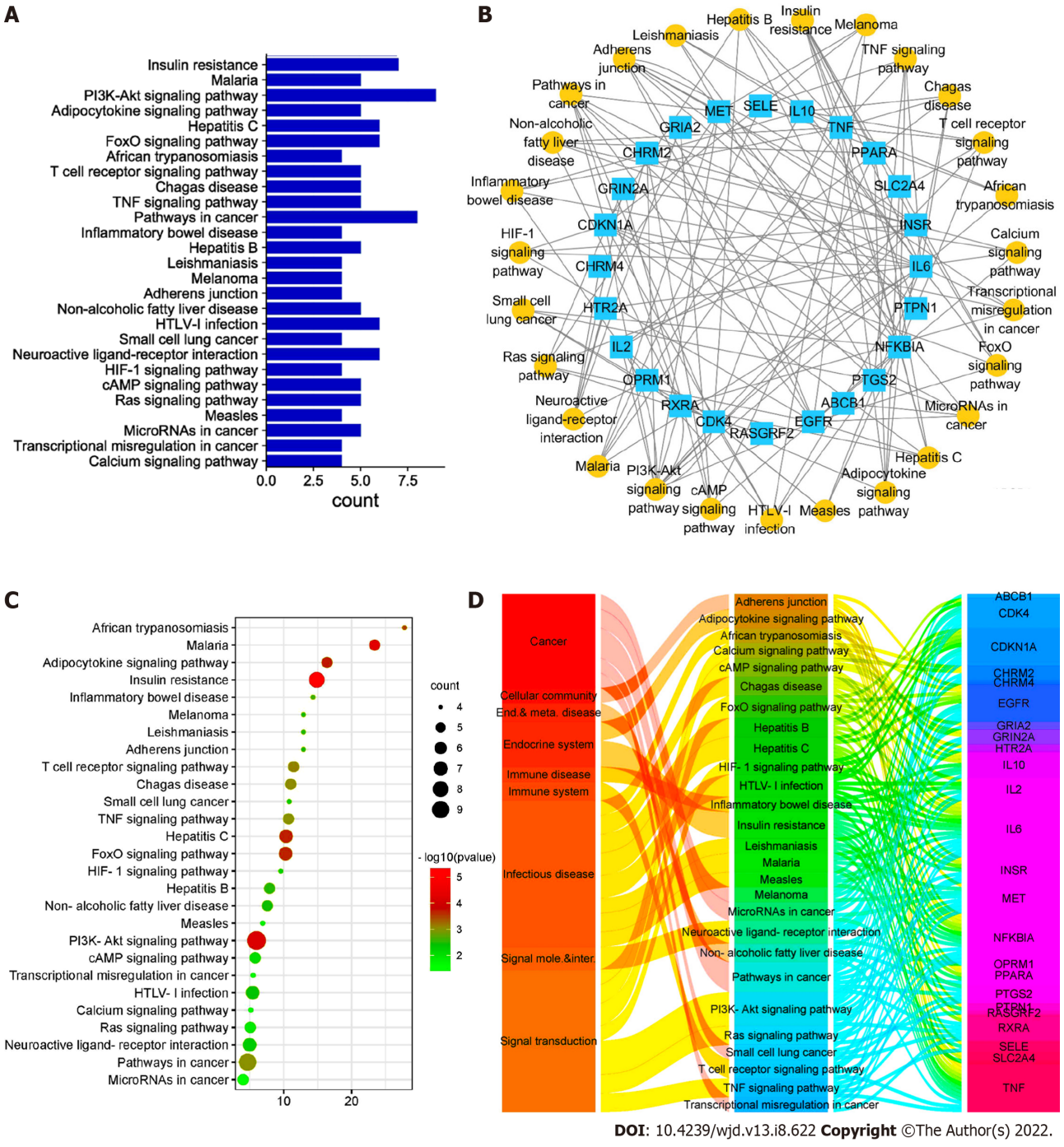


**DOI**: 10.4239/wjd.v13.i8.622 **Copyright** ©The Author(s) 2022.

**Figure 7 Target-pathway diagram of Ruyi Jinhuang powder-diabetic foot ulcer.** A: A bar graph of Kyoto Encyclopedia of Genes and Genomes (KEGG) signal pathway enrichment. The left side is the pathway name, and the right side is the number of targets contained; B: The target-path network relationship diagram. The yellow circle represents 27 pathways, and the blue square represents 36 targets; C: An enriched bubble diagram of the KEGG signaling pathway. The left side is the pathway name, and the abscissa is the fold enrichment. The bubble size corresponds to the number of targets contained, and the color category corresponds to the *P* value; D: The correspondence diagram of pathway categories. The first column is the ownership of the pathway, the second column is the pathway, and the third column is the target.

how this pathway affects DFU and needs further study.

## CONCLUSION

RHP, a traditional Chinese medicine formula, may play a role in the treatment of DFU through these target pathways by affecting insulin resistance, altering the nervous system and immune system, participating in inflammatory responses, and regulating cell proliferation, differentiation and apoptosis through other specific mechanisms. The key active components were luteolin, methyl palmitate, ar-

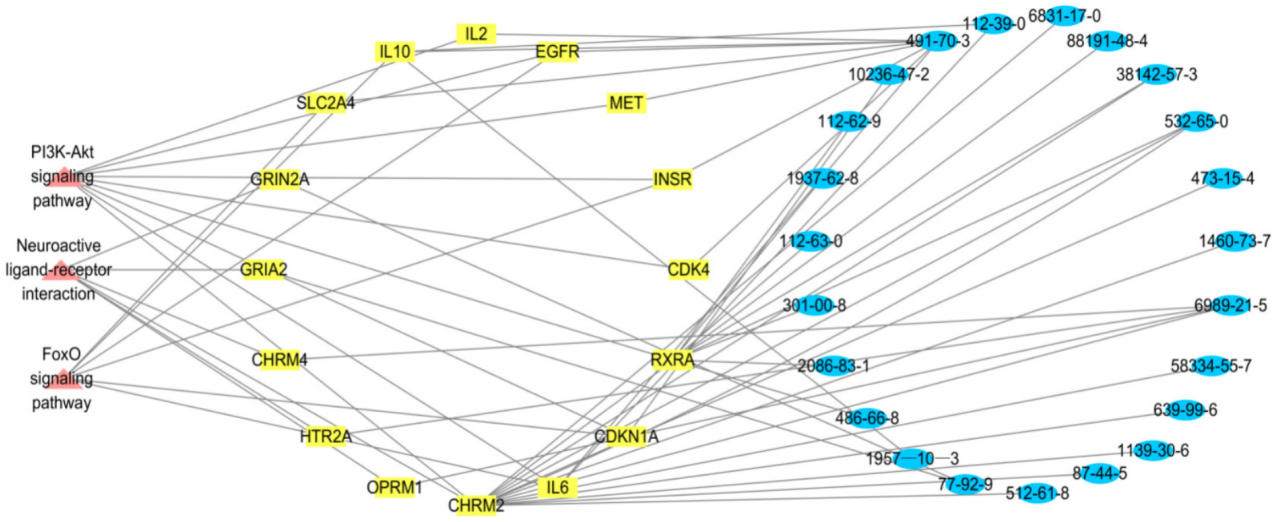


**DOI**: 10.4239/wjd.v13.i8.622 **Copyright** ©The Author(s) 2022.

**Figure 8 Critical pathway-target-component network relationship diagram of Ruyi Jinhuang powder.** Pink represents the pathway, yellow represents the target and blue represents the components. It was shown that Muscarinic Acetylcholine receptor M2 and Retinoid X Receptor alpha are common targets of the three pathways. Luteolin, atractylenone and arylodone are the key components in the three pathways.

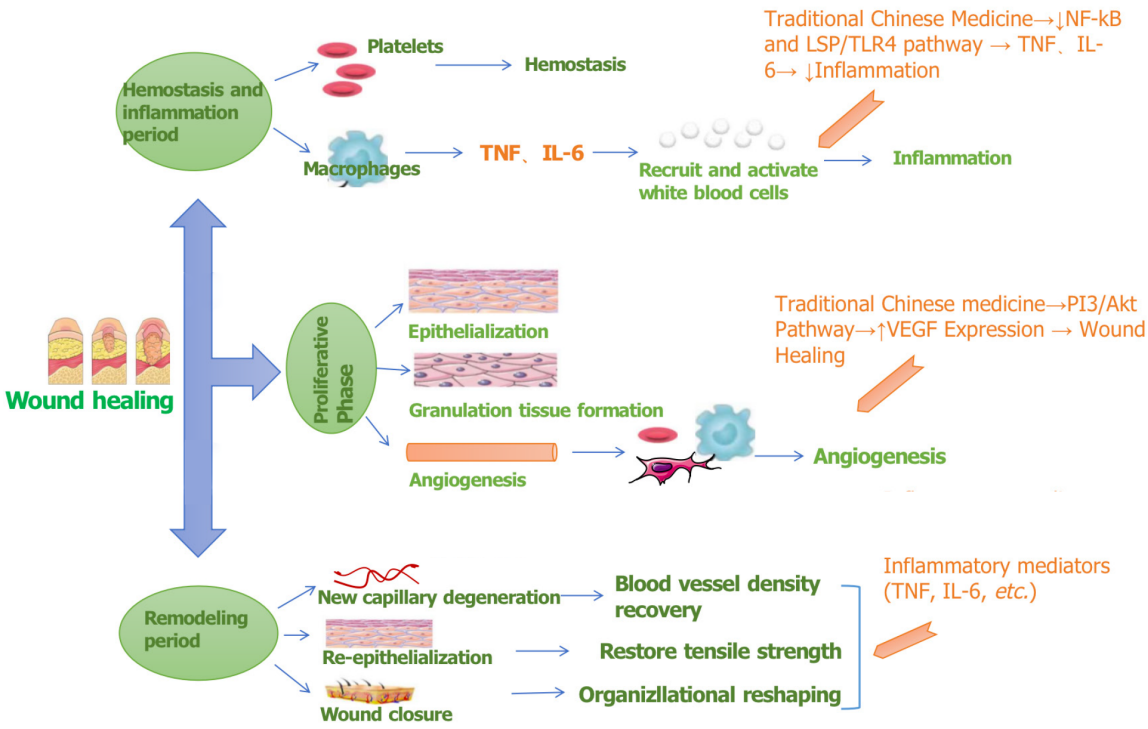


**DOI**: 10.4239/wjd.v13.i8.622 **Copyright** ©The Author(s) 2022.

**Figure 9 Wound healing mechanism diagram.** TNF: Tumor necrosis factor; IL: Interleukin; VEGF: Vascular endothelial growth factor; NF-kB: Nuclear factor-kappaB.

turmeric, methyl linoleate, palmitic acid, demethoxycurcumin, and naringin.

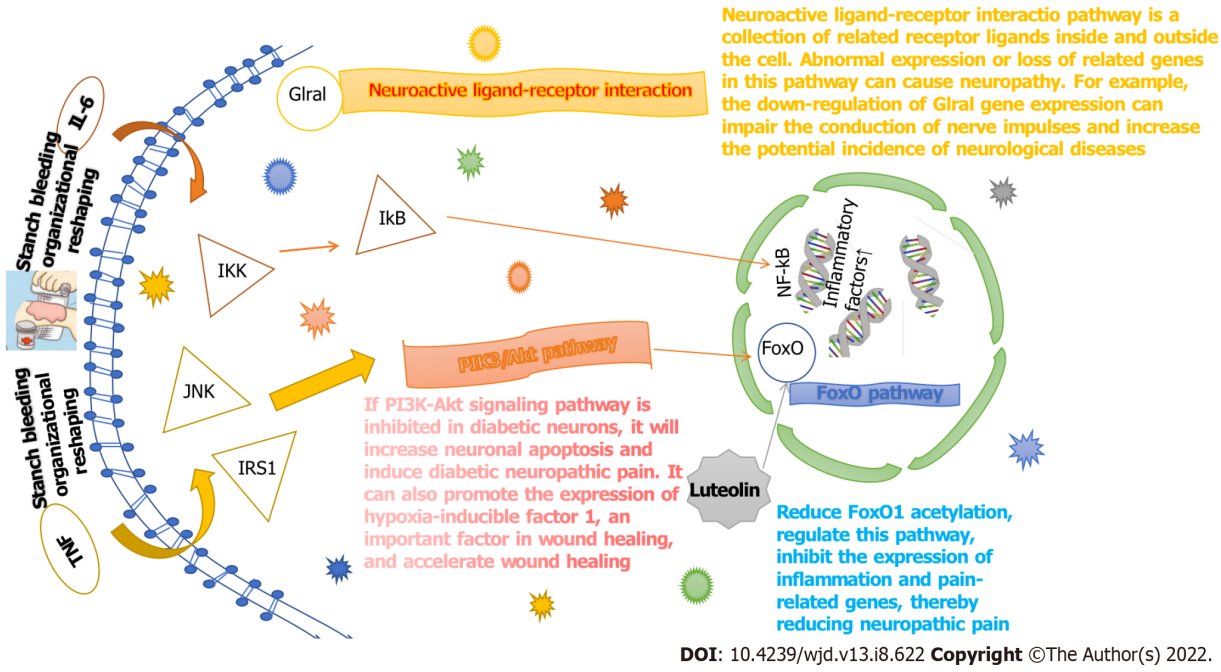


**DOI**: 10.4239/wjd.v13.i8.622 

**Figure 10 Target pathway mechanism of Ruyi Jinhuang powder.** TNF: Tumor necrosis factor; IL: Interleukin; NF-kB: Nuclear factor-kappaB; IKK: IkappaB kinase; JNK: c-Jun N-terminal kinase; IkB: Inhibitor kB; IRS1: Insulin receptor substrate-1.

## ARTICLE HIGHLIGHTS

### *Research background*

Diabetic foot ulcer (DFU) seriously affects the quality of life of patients. Traditional Chinese medicine has a unique effect in the treatment of skin ulcerative diseases. Ruyi Jinhuang powder (RHP) is one of the classic prescriptions in traditional Chinese medicine and is widely used in clinical practice.

### *Research motivation*

Although there have been studies suggesting that RHP has a therapeutic effect on DFU, there is a lack of research that further verify the mechanism of RHP to promote wound healing.

### *Research objectives*

The effective components of RHP were extracted and identified by chromatography-mass spectrometry, and the obtained chemical components were analyzed by network pharmacology methods to predict its therapeutic mechanism. Gas chromatography–mass spectrometry (MS) and ultra-performance liquid chromatography-MS were used to separately identify the chemical constituents.

### *Research methods*

Sprague Dawley rats were injected with streptozotocin to establish the DFU model. Hematoxylin-eosin staining was used to observe the wound tissue under an electron microscope. Medicine Systems Pharmacology database to obtain the target information, and the molecular docking of important components and key targets was performed in Discovery Studio software. Cytoscape software was used to visualize and analyze the relationship between the chemical composition, targets and Traditional Chinese Medicine network.

### *Research results*

RHP was shown to promote the healing of diabetic foot ulcers in rats by affecting fibroblasts and nerve cells. A total of 89 chemical components were obtained by chromatography-mass spectrometry. Network pharmacological analysis revealed that RHP was associated with 36 targets and 27 pathways in the treatment of DFU.

### *Research conclusions*

Our results indicated that RHP may play a role in the treatment of DFU through these target pathways by affecting insulin resistance, altering the nervous system and immune system, participating in inflammatory responses and regulating cell proliferation, differentiation and apoptosis and through other specific mechanisms.

### *Research perspectives*

We found that RHP plays a role in the treatment of diabetic foot ulcers through multiple targets and channels. However, the way in which specific components are combined with target proteins needs to be further explored.

## FOOTNOTES

**Author contributions:** Li XY, Zhang XT, Jiao YC, Chi H, Xiong TT and Zhang WJ, Li MN performed the experiments and acquired and analyzed the data; Li XY, Zhang XT and Wang YH wrote the manuscript; all authors approved the final version of the article.

**Supported by** National Natural Science Foundation of China, No. 82074025; Scientific Research Project of Heilongjiang Health Committee, No. 2020-293; and Scientific and Technological Innovation Project for College Students of Heilongjiang University of Chinese Medicine, No. 2021-13.

**Institutional review board statement:** This study does not involve human.

**Institutional animal care and use committee statement:** This study was approved by Ethics Committee of Heilongjiang University of Chinese Medicine, Harbin, China.

**Conflict-of-interest statement:** All the authors report no relevant conflicts of interest for this article.

**Data sharing statement:** No additional data are available.

**ARRIVE guidelines statement:** The authors have read the ARRIVE guidelines, and the manuscript was prepared and revised according to the ARRIVE guidelines.



**Country/Territory of origin:** China

**ORCID number:** Yan-Hong Wang 0000-0003-2092-2400.

**S-Editor:** Fan JR
**L-Editor:** A
**P-Editor:** Chen YX

## REFERENCES

1 **Chen SG**. Surgery Zhengzong. Beijing: People's Medical Publishing House, 2007: 345
2 **Zhang SQ**, Zeng CH, Chen C, Wei L. Modern research progress of Ruyi Jinhuang Powder. *Zhongchengyao* 2018; **40**: 411-415 [DOI: 10.3969/j.issn.1001-1528.2018.02.032]
3 **Sun D**, Zhao YD, Hu MY, Li WB, Yan XN. The application of Ruyi Jinhuang Powder in dermatology. *Linchuangyixue Yanjiu Yu Shijian* 2020; **17**: 194-196 [DOI: 10.19347/j.cnki.2096-1413.202017072]
4 **Bandyk DF**. The diabetic foot: Pathophysiology, evaluation, and treatment. *Semin Vasc Surg* 2018; **31**: 43-48 [PMID: 30876640 DOI: 10.1053/j.semvascsurg.2019.02.001]
5 **Wang XH**, Lang R, Liang Y, Zeng Q, Chen N, Yu RH. Traditional Chinese Medicine in Treating IgA Nephropathy: From Basic Science to Clinical Research. *J Transl Int Med* 2021; **9**: 161-167 [PMID: 34900626 DOI: 10.2478/jtim-2021-0021]
6 **Shao Y**, Han XL, Wang JJ. External application of Ruyi Jinhuang Powder combined with antibiotics in the treatment of 30 cases of diabetes with erysipelas in lower limbs. *Neimenggu Zhongyiyao* 2015; **9**: 68-69 [DOI: 10.16040/j.cnki.cn15-1101.2015.09.083]
7 **Liu XY**, Li YQ, Wang XZ, Zhao PT, Liu J, Zhang ZH, Li J, Gao LH, Jia N, Zhang CL. External application of Ruyi Jinhuang Powder to treat 20 cases of diabetes with skin abscess. *Henan Zhongyi* 2014; **34**: 1996-1997 [DOI: 10.16367/j.issn.1003-5028.2014.10.059]
8 **Zhang D**. Observation on the clinical efficacy of oral administration of Simiao Tongluo Decoction combined with external application of Ruyi Jinhuang Powder in the treatment of diabetic foot with damp-heat injection. *Huabei Ligong Daxue* 2020 [DOI: 10.27108/d.cnki.ghelu.2020.000812]
9 **Kibble M**, Saarinen N, Tang J, Wennerberg K, Mäkelä S, Aittokallio T. Network pharmacology applications to map the unexplored target space and therapeutic potential of natural products. *Nat Prod Rep* 2015; **32**: 1249-1266 [PMID: 26030402 DOI: 10.1039/c5np00005j]

10 **Zhang YF**, Huang Y, Ni YH, Xu ZM. Systematic elucidation of the mechanism of geraniol *via* network pharmacology. *Drug Des Devel Ther* 2019; **13**: 1069-1075 [PMID: 31040644 DOI: 10.2147/DDDT.S189088]

11 **Davis AP**, Grondin CJ, Johnson RJ, Sciaky D, Wiegers J, Wiegers TC, Mattingly CJ. Comparative Toxicogenomics Database (CTD): update 2021. *Nucleic Acids Res* 2021; **49**: D1138-D1143 [PMID: 33068428 DOI: 10.1093/nar/gkaa891]

12 **Calvier FÉ**, Bousquet C. Integrating the Comparative Toxicogenomic Database in a Human Pharmacogenomic Resource. *Stud Health Technol Inform* 2020; **270**: 267-271 [PMID: 32570388 DOI: 10.3233/SHTI200164]

13 **Tang HY**, Jiang AJ, Ma JL, Wang FJ, Shen GM. Understanding the Signaling Pathways Related to the Mechanism and Treatment of Diabetic Peripheral Neuropathy. *Endocrinology* 2019; **160**: 2119-2127 [PMID: 31318414 DOI: 10.1210/en.2019-00311]

14 **Dixon D**, Edmonds M. Managing Diabetic Foot Ulcers: Pharmacotherapy for Wound Healing. *Drugs* 2021; **81**: 29-56 [PMID: 33382445 DOI: 10.1007/s40265-020-01415-8]

15 **Feng J**, Dong C, Long Y, Mai L, Ren M, Li L, Zhou T, Yang Z, Ma J, Yan L, Yang X, Gao G, Qi W. Elevated Kallikrein-binding protein in diabetes impairs wound healing through inducing macrophage M1 polarization. *Cell Commun Signal* 2019; **17**: 60 [PMID: 31182110 DOI: 10.1186/s12964-019-0376-9]

16 **Theocharidis G**, Baltzis D, Roustit M, Tellechea A, Dangwal S, Khetani RS, Shu B, Zhao W, Fu J, Bhasin S, Kafanas A, Hui D, Sui SH, Patsopoulos NA, Bhasin M, Veves A. Integrated Skin Transcriptomics and Serum Multiplex Assays Reveal Novel Mechanisms of Wound Healing in Diabetic Foot Ulcers. *Diabetes* 2020; **69**: 2157-2169 [PMID: 32763913 DOI: 10.2337/db20-0188]

17 **Sun HS**. RXRA has a negative regulatory effect on glucose-stimulated insulin secretion Study on the regulation of pancreatic β-cell function by nuclear receptor RXRα. In: CNKI.net [Internet]. [cited 10 March 2022]. Available from: https://kns.cnki.net/kcms/detail/detail.aspx?FileName=1019055238.nh&DbName=CMFD2020

18 **Bradley SJ**, Tobin AB, Prihandoko R. The use of chemogenetic approaches to study the physiological roles of muscarinic acetylcholine receptors in the central nervous system. *Neuropharmacology* 2018; **136**: 421-426 [PMID: 29191752 DOI: 10.1016/j.neuropharm.2017.11.043]

19 **Chen J**, Cheuk IWY, Shin VY, Kwong A. Acetylcholine receptors: Key players in cancer development. *Surg Oncol* 2019; **31**: 46-53 [PMID: 31536927 DOI: 10.1016/j.suronc.2019.09.003]

20 **Yeh YH**, Hsiao HF, Yeh YC, Chen TW, Li TK. Inflammatory interferon activates HIF-1α-mediated epithelial-to-mesenchymal transition *via* PI3K/AKT/mTOR pathway. *J Exp Clin Cancer Res* 2018; **37**: 70 [PMID: 29587825 DOI: 10.1186/s13046-018-0730-6]

21 **Zheng XD**, Huang Y, Li H. Regulatory role of Apelin-13-mediated PI3K/AKT signaling pathway in the glucose and lipid metabolism of mouse with gestational diabetes mellitus. *Immunobiology* 2021; **226**: 152135 [PMID: 34521048 DOI: 10.1016/j.imbio.2021.152135]

22 **Cai SY**, Li YY. Study on the mechanism of mulberry leaf extract regulating IRS-1/PI3K/GLUT4 pathway and affecting insulin resistance in type 2 diabetes. *Xinzhongyi* 2020; **52**: 1-6 [DOI: 10.13457/j.cnki.jncm.2020.01.001]

23 **Bathina S**, Das UN. Dysregulation of PI3K-Akt-mTOR pathway in brain of streptozotocin-induced type 2 diabetes mellitus in Wistar rats. *Lipids Health Dis* 2018; **17**: 168 [PMID: 30041644 DOI: 10.1186/s12944-018-0809-2]

24 **Kim JH**, Bae HC, Kim J, Lee H, Ryu WI, Son ED, Lee TR, Jeong SH, Son SW. HIF-1α-mediated BMP6 down-regulation leads to hyperproliferation and abnormal differentiation of keratinocytes in vitro. *Exp Dermatol* 2018; **27**: 1287-1293 [PMID: 30230035 DOI: 10.1111/exd.13785]

25 **Lauss M**, Kriegner A, Vierlinger K, Noehammer C. Characterization of the drugged human genome. *Pharmacogenomics* 2007; **8**: 1063-1073 [PMID: 17716238 DOI: 10.2217/14622416.8.8.1063]

26 **Yang XY**. Changes in gene expression of the neural activity ligand-receptor interaction pathway in the brain tissue of IVM mice can lead to abnormal gene expression in the second generation of paternal offspring. *Zhejiang University* 2016; 1-67

27 **Liang MD**, Yang XY, Du GH. Research progress in the mechanism of type 2 diabetes inducing skeletal muscle atrophy and the effect of commonly used hypoglycemic drugs. *Yaoxue Xuebao* 2021; **57**: 568-575 [DOI: 10.16438/j.0513-4870.2021-1217]

28 **Hua GF**, Jin HF, Lu C, Guo XW. The effect of intraperitoneal injection of luteolin to regulate the Sirt1/FOXO1 pathway on pain sensitization in rats with chronic sciatic nerve ligation. *Zhejiang Yixue* 2021; **43**: 1489-1512 [DOI: 10.12056/j.issn.1006-2785.2021.43.14.2021-971]

Published by **Baishideng Publishing Group Inc**
7041 Koll Center Parkway, Suite 160, Pleasanton, CA 94566, USA
**Telephone:** +1-925-3991568
**E-mail:** bpgoffice@wjgnet.com
**Help Desk:** https://www.f6publishing.com/helpdesk
https://www.wjgnet.com